Available online at www.sciencedirect.com
ScienceDirect
Journal of Membrane Science 287 (2007) 246–256
journal of MEMBRANE SCIENCE
www.elsevier.com/locate/memsci

Asymmetric bipolar membrane: A tool to improve product purity

J. Balster [a], R. Sumbharaju [b], S. Srikantharajah [b], I. Pünt [a], D.F. Stamatialis [a,*], V. Jordan [b], M. Wessling [a]

[a] *University of Twente, Membrane Technology Group, Faculty of Science and Technology, Postbus 217, 7500 AE Enschede, The Netherlands*
[b] *Department of Chemical Engineering, Fachhochschule Münster, University of Applied Sciences, Stegewaldstrasse 39, 48565 Steinfurt, Germany*

Received 16 August 2006; received in revised form 20 October 2006; accepted 24 October 2006
Available online 6 November 2006

Abstract

Bipolar membranes (BPMs) are catalytic membranes for electro-membrane processes splitting water into protons and hydroxyl ions. To improve selectivity and current efficiency of BPMs, we prepare new asymmetric BPMs with reduced salt leakages. The flux of salt ions across a BPM is determined by the co-ion transport across the respective layer of the membrane. BPM asymmetry can be used to decrease the co-ion fluxes through the membrane and shows that the change of the layer thickness and charge density of the corresponding ion exchange layer determines the co-ion flux. The modification of a commercial BP-1 with a thin additional cation exchange layer on the cationic side results in a 47% lower salt leakage. Thicker layers result in water diffusion limitations. In order to avoid water diffusion limitations we prepared tailor made BPMs with thin anion exchange layers, to increase the water flux into the membrane. Therefore a BPM could be prepared with a thick cation exchange layer showing a 62% decreased salt ion leakage through the cationic side of the membrane.

Keywords: Bipolar membrane; Asymmetry; Electrodialysis; Salt leakage

1. Introduction

A bipolar membrane (BPM), a laminate of a cation (CEL) and an anion exchange layer (AEL), allows the electro-dissociation of water into hydroxide ions and protons without the generation of gases (Fig. 1a). BPMs are small chemical reactors with integrated separation, which allow the design of unique processes like the production and recovery of acids and bases, the variation of the pH of a process stream, and the separation of proteins [1].

The anion and cation selective layers of a BPM should allow the selective transport of the protons and hydroxyl ions out of the transition region into the acid and base chamber and block co-ions from reaching the contact region and the opposite side of the membrane (Fig. 1a, full arrows). In addition, the layers should allow sufficient water flux into the BPM to replenish the water consumed by the water dissociation reaction [2]. In bipolar membrane electrodialysis (ED-BPM), the BPM is stacked together with monopolar anion and cation exchange membranes into a membrane module to produce acids and bases from their corresponding salts (Fig. 1b). The salt solution is fed to the central compartment, and the ions migrate out of this compartment into the neighbouring ones (Fig. 1b, full arrows). Charge compensation because of electro-neutrality occurs due to the water splitting at the interface of the BPMs [1]. The produced acid and base are in contact with the cation and anion permeable layer of the BPM (Fig. 1b). BPMs are not only permeable to the water splitting products, but to acid anions and base cations, as well. These ions are transported across the bipolar membrane junction to the other ion permeable layer, where they are transported as counter-ions (co-ion leakage) (Fig. 1a, dotted arrows) resulting in salt impurities of the products of EDBPM processes (Fig. 1b, dotted arrows) [3].

Fig. 2 presents a typical steady state current density–voltage drop (i–v) curves of a BPM for a neutral salt solution (M^+X^-) starting out of the salt form of the BPM [4,5]. Below the first limiting current density (i_{lim1}) the current is only transported by salt ions. At i_{lim1}, the electrical resistance increases significantly since all salt ions are removed from the BPM junction. The magnitude of i_{lim1} is a measure for the selectivity of the BPM towards co-ion leakage [4]. The salt ion fluxes measured in acid–base electrodialysis are closely related to the salt ion fluxes during measurements in salt solutions [4]. Therefore the

* Corresponding author. Tel.: +31 53 4894675; fax: +31 53 4894611.
E-mail address: d.stamatialis@utwente.nl (D.F. Stamatialis).

0376-7388/$ – see front matter © 2006 Elsevier B.V. All rights reserved.
doi:10.1016/j.memsci.2006.10.042

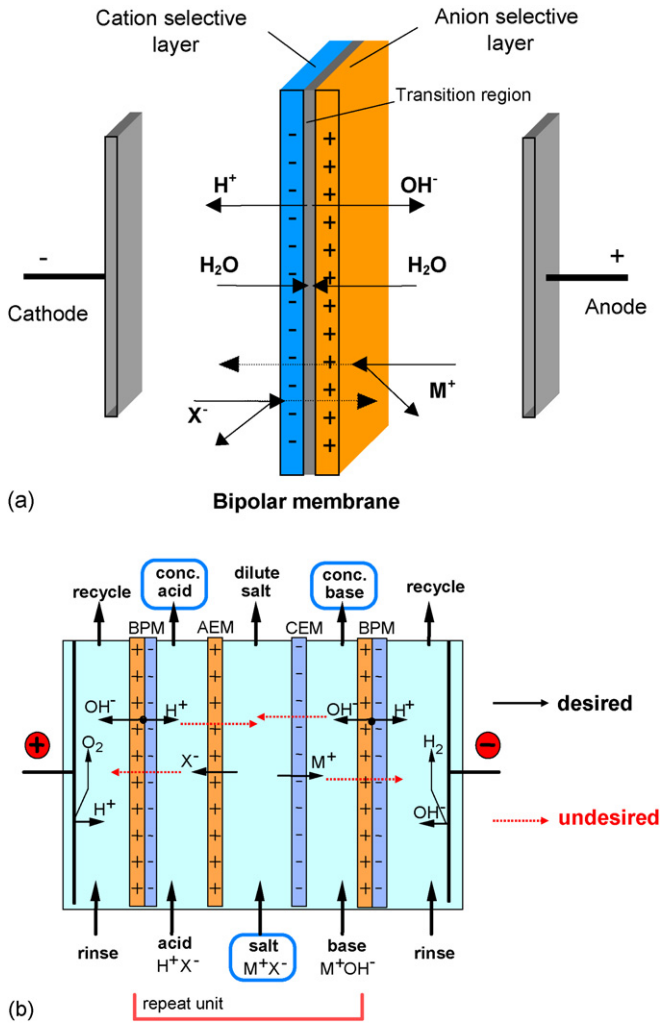

Fig. 1. (a) Water splitting function of a BPM and (b) schematic drawing of a membrane module for the production of acids and bases, indicating the ion and the co-ion transport.

i_{lim1} of different membranes can be used to predict and compare their co-ion leakage.

Above U_{diss}, water splitting occurs and the products (J_{OH^-}/J_{H^+}) are also available for the current transport resulting in a steep increase in i above i_{lim1} [5]. The operating current density (i_{op}) should be as high as possible to reduce the relative salt

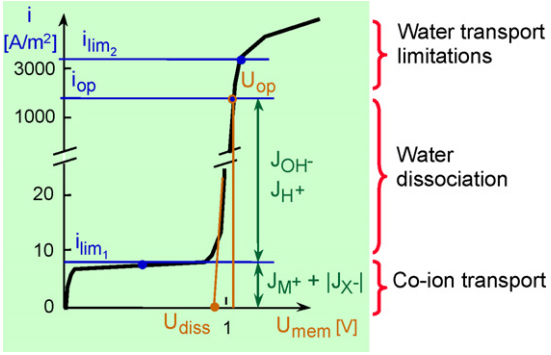

Fig. 2. Schematic i–v curve of a BPM in a salt solution (M^+X^-), adapted from [4,5].

ion transport and to have a high water splitting efficiency. Above the second limiting current (i_{lim2}) the water transport toward the BPM junction is not sufficient to replenish the water dissociated at the interface, leading to water diffusion limitations and therefore to a dry out of the membrane [6,7].

The total salt ion transport across commercial BPMs is generally over 0.01 $mol_{salt}/mol_{H^+/OH^-}$ when the concentration of the produced acids and/or base is above 4 mol/L [8,9]. Therefore concentrated acids and bases with purity higher than 99 mol% (of dissolved ions) cannot be produced. ED-BPM can only become competitive for many industrial applications, if the salt impurity in the product is reduced drastically [4]. In general, the salt ion leakage into the produced acids and bases is not the same in both directions [8,10,11]. Hence, BPMs show an asymmetric salt ion transport behaviour depending on the transport properties of the ion exchange layers [11]. In fact, the flux of salt ions across the BPM is determined by the co-ion transport across the respective membrane layer [4].

Wilhelm et al. [4,5] have already shown that an improvement of the composition of one of the two layers [4] and an increase of layer thickness [5] can lead to an enhanced selectivity and therefore to a reduced salt ion leakage. However, if the properties of the second ion exchange layer (IEL) are not optimised, water transport limitations occur. Such a thickness dependence of the membrane selectivity has not been reported for standard ion exchange membranes [4].

In this work, we prepare new asymmetric BPMs by optimising the properties and/or increasing the thickness of one of the two charged layers until nearly no water transport occurs through this side of the membrane. In order to avoid water transport limitation to the interface layer as well, the thickness of the other ion exchange layer is reduced. Our experimental study expands into two different directions:

(1) Modification of the commercial BP-1 membrane (Tokuyama Soda). In fact the thickness of the anion or cation exchange layer is increased by lamination of either:
   - commercial anion (AMX) and cation (CMX) membranes (Tokuyama Soda) or
   - tailor made cation exchange membranes of polymer blends of sulphonated poly(ether ether ketone) (S-PEEK) and poly(ether sulphone) (PES).

(2) Preparation of tailor made asymmetric BPMs using polymer blends of S-PEEK/PES as cation exchange material and functionalised poly(sulphone) (Psf) as anion exchange material. In this case, the properties of both ion exchange layers can be modified in order to avoid water diffusion limitations.

2. Theoretical background

The flux of salt ions (J_i) across the BPM can be described with the actual transport number (t_i) and the operational current density (i_{op}) [4]:

$$J_i = t_i \frac{i_{op}}{z_i F}, \quad (1)$$

where F is the Faraday constant and z_i is the electrochemical valence of the ion. If boundary layer effects in the salt solutions next to the membrane are neglected, the co-ion concentration in the membrane will remain constant at the solution interface, even with increased ion fluxes. Assuming no influence of the water splitting in the bipolar membrane interface on the salt ion transport across the BPM, the salt ion fluxes at the i_{op} and at i_{lim1} are the same [4]:

$$J_i = J_i^{i_{lim\,1}} = t_i^{i_{lim1}} \frac{i_{lim\,1}}{z_i F}. \quad (2)$$

The i_{lim1} of a BPM can also be written as:

$$i_{lim\,1} = F(Z_{M^+} J_{M^+} + Z_{X^-} J_{X^-}), \quad (3)$$

where M^+ is the salt cation and X^- is the salt anion (see Fig. 2).

The salt ion flux J_i in a BPM with equal salt concentrations at the anionic and cationic membrane sides can be described by the extended Nernst-Plack equations. These equations are phenomenological descriptions of the ion transport by diffusion due to a concentration gradient and migration due to an electrical field. Neglecting convective transport and bulk movement of the solution the ion flux can be described as [4]:

$$J_i = J_i^{Diffusion} + J_i^{Migration} = -D_i \frac{dc_i}{dx} - D_i \frac{c_i z_i F}{RT} \frac{dU}{dx}, \quad (4)$$

where D_i is the ionic diffusion coefficient, c_i the ion concentration, R the gas constant, T the actual temperature, U the electric potential and x is the location normal to the membrane. Assuming linear concentration profiles at steady state conditions at low current densities and constant electric field strength across the membrane layer, the use of an average concentration is required in the migrational term to describe the transport at steady state. Therefore the average concentration in the membrane layer at the solution interface and the inner membrane interface is used [4]. The co-ion leakage through the AEL can be written as:

$$J_{M^+} = -D^m_{M^+,AEL} \frac{\Delta c^m_{M^+}}{d_{wet,AEL}} - D^m_{M^+,AEL} \frac{c^{m,av}_{M^+} F}{RT} \frac{\Delta U_{AEL}}{d_{wet,AEL}}, \quad (5)$$

and

$$J_{X^-} = -D^m_{X^-,CEL} \frac{\Delta c^m_{X^-}}{d_{wet,CEL}} - D^m_{X^-,CEL} \frac{c^{m,av}_{X^-} F}{RT} \frac{\Delta U_{CEL}}{d_{wet,CEL}}, \quad (6)$$

for the CEL, with d_{wet} as the wet thickness of the membrane layer. The superscripts 'm' and 'av' denote the membrane phase and average value across this phase, respectively.

At i_{lim1} the co-ion concentration at the inner interface is zero and the co-ion concentration difference across a layer is equal to the co-ion concentration next to the solution. This difference equals the concentration difference of the counter ions due to electroneutrality requirement. At i_{lim1} the arithmetic averages of the co- and counter-ion concentrations in the IELs become [4]:

$$c^{m,av}_{M^+} = 0.5 c^s_{M^+,AEL} \quad \text{(in the AEL)}, \quad (7)$$

and

$$c^{m,av}_{X^-} = 0.5 c^s_{X^-,CEL} \quad \text{(in the CEL)}, \quad (8)$$

where the superscript 's' denotes the layer next to the solution. Taking the electroneutrality in the membrane into account, the arithmetic average of the counter ion concentration in the IELs are:

$$c^{m,av}_{X^-} = c^{m,av}_{M^+} + c_{char,AEL} = 0.5 c^s_{M^+,AEL} + c_{char,AEL} \quad \text{(in the AEL)}, \quad (9)$$

and

$$c^{m,av}_{M^+} = c^{m,av}_{X^-} + c_{char,CEL} = 0.5 c^s_{X^-,CEL} + c_{char,CEL} \quad \text{(in the CEL)}, \quad (10)$$

where c_{char} is the charge density of the corresponding IEL [4].

By introducing the averages and differences into the Nernst-Plack equations and eliminating the potential drop across the IELs (it is the same for anion and cation flux equation) the Nernst-Planck equations for the ion fluxes at i_{lim1} (J_i^{lim}) can be simplified [4]. Because the ion fluxes in steady state have to be the same in both layers of the BPM the ion fluxes can be described by the following equations:

$$J^{lim}_{M^+} = \frac{D_{M^+,AEL}}{d_{wet,AEL} c_{char,AEL}} (c^s_{M^+,AEL} + c_{char,AEL}) c^s_{M^+,AEL}, \quad (11)$$

$$J^{lim}_{X^-} = \frac{D_{X^-,CEL}}{d_{wet,CEL} c_{char,CEL}} (c^s_{X^-,CEL} + c_{char,CEL}) c^s_{X^-,CEL}. \quad (12)$$

To relate the content of co- and counter ions in the membrane to the concentration in the electrolyte solution the Donnan equilibrium is used leading to a further simplification of the ion transport equations [4]:

$$J^{lim}_{M^+} = \frac{D_{M^+,AEL} (c^s)^2}{d_{AEL} c_{char,AEL}}, \quad (13)$$

$$J^{lim}_{X^-} = \frac{D_{X^-,CEL} (c^s)^2}{d_{wet,CEL} c_{char,CEL}}. \quad (14)$$

By inserting Eqs. (13) and (14) into Eq. (3) the first limiting current density can be expressed as:

$$i_{lim1} = F \left(\frac{D_{M^+,AEL} (c^s)^2}{d_{wet,AEL} c_{char,AEL}} + \frac{D_{X^-,CEL} (c^s)^2}{d_{wet,CEL} c_{char,CEL}} \right). \quad (15)$$

The i_{lim1} and the salt transport across a BPM are directly dependent on the square of the solution concentration, the diffusion coefficients in the membrane layers, the fixed charge density and thickness of the IELs of the BPM.

Wilhelm et al. [4,5] developed models to simulate ion fluxes through BPMs and to relate them to i_{lim1} using either a symmetrical (assuming that the transport in both layers is the same) or an asymmetrical (assuming different transport in the two layers) approach. The measurements and simulations showed [4,5], that both the anionic and the cationic co-ion leakage change, if one of the two layers of the BPM is changed.

In this study, we assume asymmetrical ion transport through the layers of the BPM, assuming that a change of one layer of the BPM reduces the ion flux through both layers symmetrically, i.e. when the Cl^- flux through the BPM is reduced about 30%

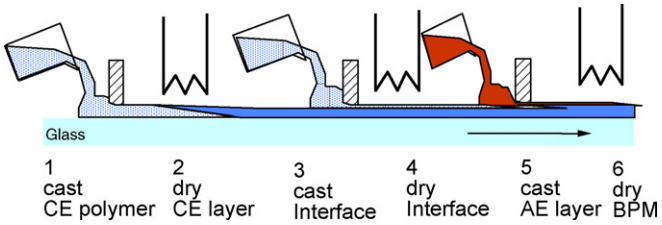

Fig. 3. Schematic drawing of the BPM preparation by the casting technique, adapted from [6].

because of a change of the CEL layer, we assume that also the Na^+ flux is reduced about 30%. With this method we can use the ratio of the measured i_{lim1} of the BPMs to estimate the co-ion fluxes.

3. Experimental

3.1. Commercial membranes

The commercial BPM Neosepta BP-1 from Tokuyama Soda Ltd. (Tokyo, Japan) was used in this study. In order to increase the asymmetry, commercially available Neosepta CMX (cation exchange) and AMX (anion exchange) membranes (also from Tokuyama Soda Ltd.), or tailor made S-PEEK/PES membranes have been laminated to the BP-1 to the corresponding side of the membrane by a frame.

3.2. Tailor made membranes

S-PEEK was prepared by sulphonation of poly(ether ether ketone) (PEEK) 450PF from Victrex as described in [12]. The S-PEEK and S-PEEK/PES blends (indicated as S/P in the text) were prepared by adding the desired amount of polymers to the solvent (NMP, 10 or 20 wt.% polymer in solution), stirred for a minimum of 24 h and filtered over a 40 μm metal filter. For the contact region of the BPM, a pure S-PEEK layer with a sulphonation degree (SD) of 80% on the cationic side and a poly(4-vinyl pyridine) (P4VP) layer were used. The AEL was prepared from aminated Psf in NMP (10 wt.% polymer in solution) obtained from FuMA-TECH GmbH (St. Ingbert, Germany).

Single ion exchange films as well as the BPMs were prepared by the evaporation technique [13]. In order to have a good contact between the different layers the casting method was used (see Fig. 3) [14]. The polymer layers were cast with the desired thickness and sequence onto a glass plate. After the solidification of one layer the next layer was cast on top of the former, which then was allowed to dry. This procedure was repeated until all desired layers (CEL, two intermediate layers, AEL) were cast onto each other. Because all polymer solutions were prepared in the same solvent, the contact at the interface layers was firm. The prepared membranes were dried in N_2 atmosphere at 40–80 °C for 1 week, then immersed in water and subsequently dried under vacuum at 30 °C for 1 week. The membranes were finally stored in a 2 M NaCl solution.

3.3. Characterisation of the ion exchange membrane layers

The commercial AMX and CMX membranes and the tailor made ion exchange membrane layers were characterised by measurements of the ion exchange capacity (IEC), water uptake (w), permselectivity (P) and electrical resistance (R). These properties were used to calculate the SD, the specific membrane conductivity (Cond), and the c_{char} of the membranes (more details in [12,13]).

3.4. Characterisation of the BPMs

The i–v curve measurements were performed in a six-compartment membrane stack as shown schematically in Fig. 4a (see more details about the procedure in [4] and the experimental setup in [15]). The central BPM was the one under investigation. The other membranes were auxiliary membranes, which were necessary to maintain well-defined, constant concentrations in the two central compartments. During the experiment, the applied current density was increased stepwise and the system was allowed to reach steady state. The voltage drop across the membrane was measured with calomel electrodes at a fixed distance from the membrane surface by Haber-Luggin capillaries filled with concentrated KCl solution, followed by the next increase in current density. The temperature was held constant at 25 °C.

Generally, in such measurements, the solution resistance is subtracted. However, because the limiting current density is not affected by the solution resistance [4] and the solution resistance close to the BPMs decreases at higher current densities because of the generation of H^+ and OH^- (the conductivity next to the membrane changes), the i–v curves in this article were not corrected for the solution resistance.

The current efficiency and the purity of the produced acids and bases are directly related to the M^+/X^- leakages through the BPM. The co-ion leakage results in product contamination and reduces the efficiency of the H^+/OH^- generation. The current efficiency of the BPMs was measured with the arrangement shown in Fig. 4b. The experiments were performed in batch mode measuring the base concentration in compartment 3 over time. The current efficiency was calculated [16] as:

$$\eta = \frac{(c_0 - c_t) \times V \times F}{I \times t}, \tag{16}$$

where c_0 and c_t are the equivalent concentration of the produced base at time 0 and t respectively, V the circulated volume of solution per compartment, and I is the applied current.

The salt ion leakage measurements were performed in a four-compartment cell configuration (Fig. 4c). A 0.5 M $NaSO_4$ solution was used as electrode solution, a 2 M NaCl solution was fed to the acid compartment and a 0.1 M NaOH solution to the base compartment. The experiments were performed in batch mode with a constant current density of 100 mA/cm^2 and the Cl^- concentration in the base compartment was measured by titration. The corresponding Cl^- flux (J_{Cl^-}) through the mem-

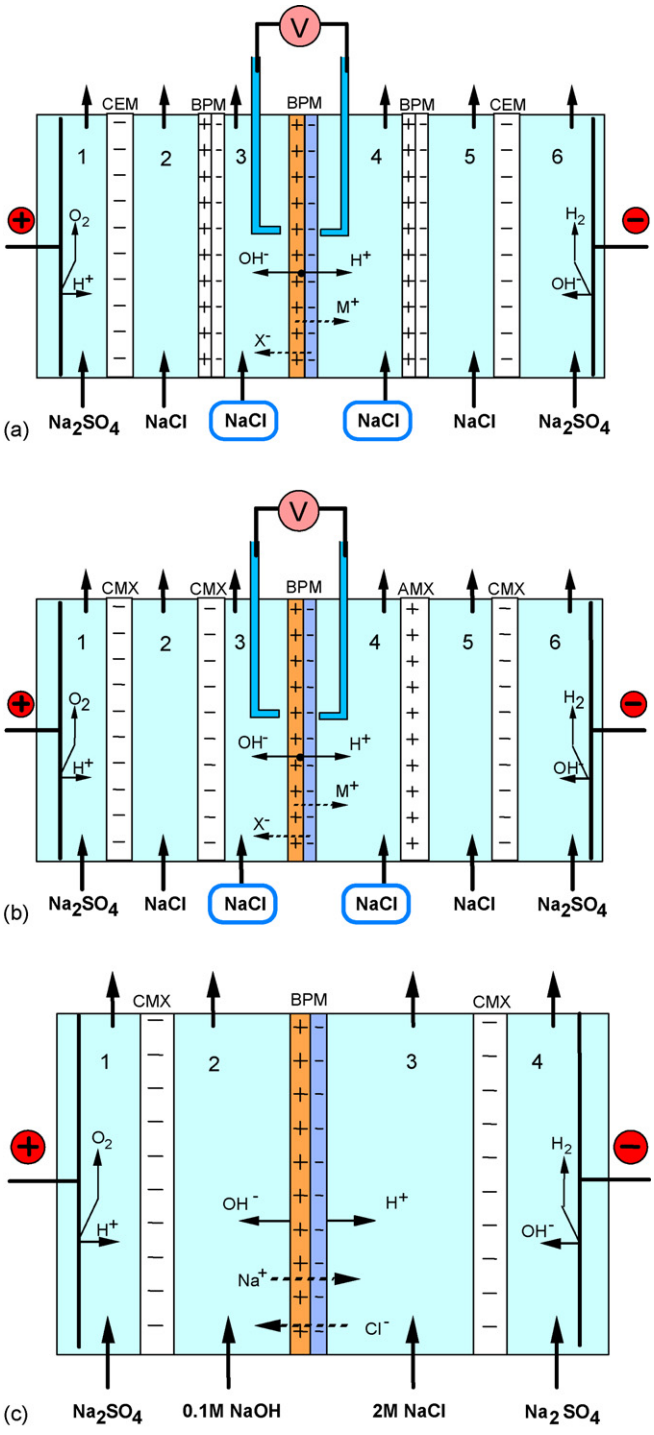

Fig. 4. Schematic drawing of: (a) a six-compartment measurement module for *i–v* curve measurements, taken from [5]; (b) a six-compartment measurement module for the efficiency measurements, adapted from [5]; (c) a four-compartment measurement module for the salt leakage determination.

brane was calculated from the change of Cl^- concentration in time (dc_{Cl^-}/dt) in the base compartment 2:

$$J_{Cl^-} = \frac{V \times (dc_{Cl^-}/dt)}{A}, \quad (17)$$

where A is the membrane area. Transport numbers of Cl^- (t_{Cl^-}) were calculated from the corresponding Cl^- fluxes:

$$t_{Cl^-} = \frac{J_{Cl^-} \times F}{i}, \quad (18)$$

where i is the applied current density.

4. Results and discussion

4.1. Modification of the commercial BP-1 membrane

4.1.1. Lamination of commercial anion (AMX) and cation (CMX) exchange layers

Table 1 presents the properties of the commercial CMX and AMX membranes laminated on the BP-1 membrane. Fig. 5

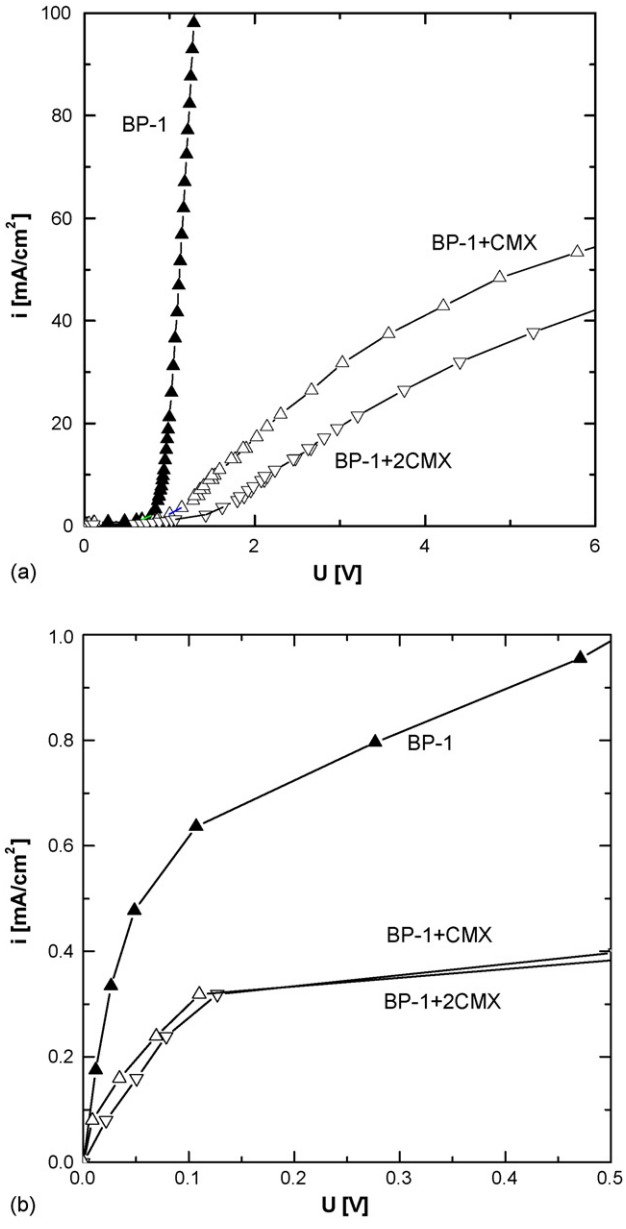

Fig. 5. *i–v* curves of BP-1 and BP-1 + CMX laminates, measured in 2 M NaCl. (a) Full curves and (b) focusing at low current density.

Table 1
Properties of the commercial ion exchange membranes

Membrane	d_{wet} (μm)	Cond (mS/cm)	IEC (mol/kg$_{dry}$)	w (kg$_{water}$/kg$_{dry}$)	c_{char} (mol/L)	P (%)
CMX	163	4.8	1.65	0.26	6.4	97
AMX	146	5.4	1.42	0.26	5.5	96

Table 2
Characteristics of the different BPM arrangements

Membrane	i_{lim1} (mA/cm^2)	i_{lim2} (mA/cm^2)	U_{diss} (V)	R_{diss} (Ω cm^2)	R_{op} (Ω cm^2)
BP-1	0.61	298	0.9	4.3	8.1
BP-1 + CMX	0.31	43	0.9	67.3	125.4
BP-1 + 2CMX	0.31	30	1.3	86.5	201.3
BP-1 + AMX	0.46	193	1.1	5.1	10.7
BP-1 + 2AMX	0.43	182	1.3	6.5	14.9

shows the effect of the lamination of CMX membranes to the cationic side of the BP-1 membrane and Table 2 presents the properties of the new BPMs. Fig. 5a presents the entire i–v curves and Fig. 5b focuses at the low current density region.

The addition of one CMX membrane leads to a significant decrease of the i_{lim1} of about 50% (from 0.61 to 0.31 mA/cm^2) corresponding to lower salt leakage through the cationic side of the membrane. The R_{op} however, increases more than 15 times from 8.1 to 125.4 Ω cm^2 (Table 2). In addition, the water transport through this membrane side is reduced and the i_{lim2} decreases sharply (see Table 2 and Fig. 5a). The addition of a second CMX layer on the cationic side of the BP-1 does not result in further decrease of i_{lim1} (Fig. 5a), it only causes further decrease of i_{lim2} and further increase in R_{op} (Table 2).

Fig. 6 presents the i–v curves of the BP-1 membrane when AMX membranes are laminated to the anionic side. In comparison to the single BP-1, the i_{lim1} decreases about 25% by the addition of one AMX membrane and 30% by the addition of two AMX membranes (see Table 2). The R_{diss} of the new membrane increases about 32% (from 4.3 to 5.1 Ω cm^2) and 84% (from 4.3 to 6.5 Ω cm^2) by the addition of one or two AMX membranes, respectively. The i_{lim2} of the new membranes decreases too (35% for the lamination of one and 37% for the lamination of two AMX membranes, see Table 2).

The results of Figs. 5 and 6 indicate that the cationic side of the BP-1 membrane contains more water and co-ions than the anionic side. Therefore the i_{lim1} and the water transport into the BP-1 can be significantly reduced by adding extra CMX membranes, leading to lower co-ion leakage, but also to water diffusion limitations.

The reduction of the co-ion leakage through the anionic side of the BP-1 membrane can be achieved by the lamination of AMX membranes. In this case, the new laminates have acceptable resistances.

4.1.2. Laminates of S-PEEK/PES blend membranes

In this section, we laminate 60 wt.% S-PEEK/40 wt.% PES blends (indicated as S/P) on the cationic side the BP-1 membrane. Table 3 presents the properties of the blends. For the preparation of the blends, we used two S-PEEK polymers with

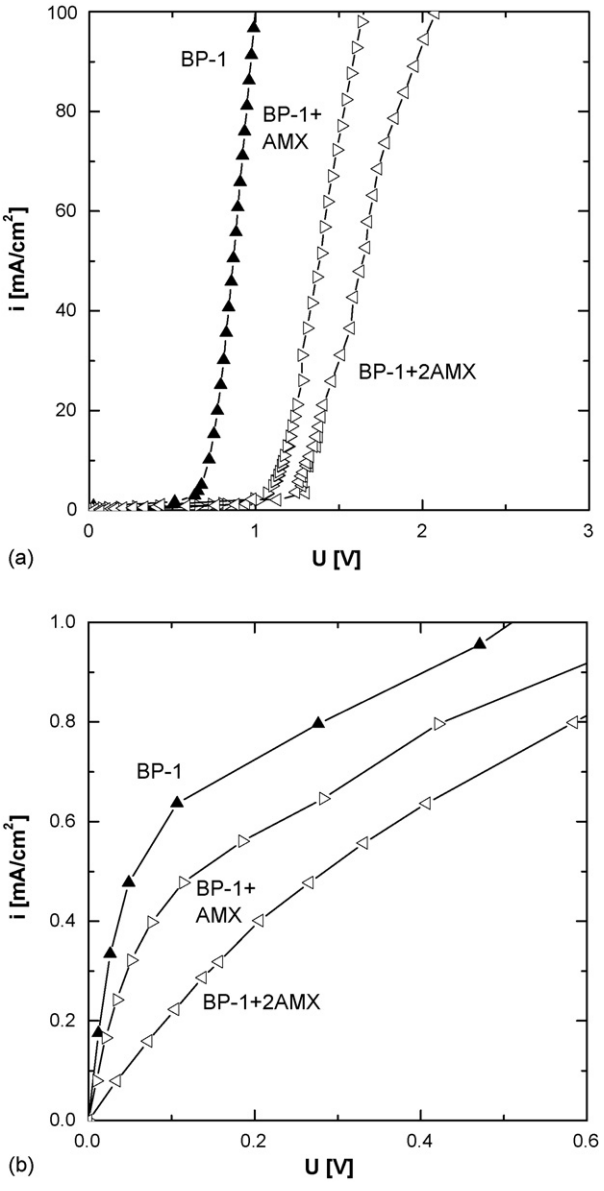

Fig. 6. i–v curves of BP-1 and BP-1 + AMX laminates, measured in 2 M NaCl. (a) Full curves and (b) focusing at low current density.

Table 3
Properties of the prepared CELs

Membrane	Blend composition	SD S-PEEK (%)	d_{wet} (μm)	Cond (mS/cm)	IEC (mol/kg_{dry})	w (kg_{water}/kg_{dry})	c_{char} (mol/L)	P (%)
S/P-3.8	60% S-PEEK, 40% PES	80	80	1.9	1.3	0.34	3.8	96
S/P-6.4	60% S-PEEK, 40% PES	62	65	0.1	0.9	0.14	6.4	97

Table 4
Characteristics of the tailor made BPM arrangements

Membrane	i_{lim1} (mA/cm^2)	i_{lim2} (mA/cm^2)	U_{diss} (V)	R_{diss} (Ω cm^2)	R_{op} (Ω cm^2)	η_{NaOH} (%)	J_{Cl^-} ($\times 10^{-9}$ mol(cm^2 s))		t_{Cl^-} (%)
							Measured	Estimated	
BP-1	0.61	298	0.90	4.3	8.1	90	5.1	–	0.49
BP-1 + S/P-3.8	0.41	217	0.95	4.4	8.7	89	3.5	3.4	0.34
BP-1 + S/P-6.4	0.32	184	0.96	5.3	10.4	89	–	2.7	0.26

SDs of 80% and 62%. Therefore we prepared blends of two different charge densities, 3.8 and 6.4 mol/L (indicated as S/P-3.8 and S/P-6.4, Table 3).

Fig. 7 shows the effect of the lamination of S/P-3.8 membranes of different thickness to the cationic side of the BP-1. Fig. 7a shows the complete i–v curve and Fig. 7b focuses on the lower current density region. The addition of the 80 μm S/P-3.8 leads to a reduction of i_{lim1} of 33% (from 0.61 to 0.41 mA/cm^2), an increase of R_{op} of only 7% (from 8.1 to 8.7 Ω cm^2) and a decrease of i_{lim2} of 27% (from 298 to 217 mA/cm^2) in comparison to the BP-1 membrane (see Table 4). The addition of a 150 μm S/P-3.8 results in water diffusion limitations (see Fig. 7a). The operable current density is reduced drastically (97%, from 298 to 9 mA/cm^2 compared to the initial BP-1 membrane and 96% compared to the thinner BP-1 S/P 3.8 laminate), whereas i_{lim1} is only reduced to 0.39 mA/cm^2.

Fig. 8 and Table 4 show the effect of the addition of S/P membranes with different charge density to the cationic side of the BP-1. Fig. 8a shows the complete i–v curve and Fig. 8b focuses at the lower current density region. The S/P-6.4 swells less in water and has lower conductivity than the S/P-3.8 (see Table 3). As a result, its lamination to the BP-1 leads to a stronger decrease of i_{lim1} (48%, from 0.61 to 0.32 mA/cm^2) higher resistance (28%, from 8.1 to 10.4 Ω cm^2) and a lower i_{lim2} of about 38%.

Table 4 also presents the leakage of Cl^- through the BP-1 and BP-1 + S/P laminates. The Cl^- flux through the BP-1 is 5.1×10^{-9} mol/(cm^2 s). When the S/P-3.8 layer is added to the BP-1, the Cl^- flux decreases to 3.5×10^{-9} mol/(cm^2 s). It is important to note, that the Cl^- flux through this membrane estimated by the change in i_{lim1} (0.61 mA/cm^2 for the BP-1 and 0.41 for the BP-1 + S/P-3.8 laminate), using Eq. (3) (assuming a symmetrical decrease of the co-ion fluxes) is 3.4×10^{-9} (mol/(cm^2 s)) and it is in excellent agreement with the measured value 3.5×10^{-9} (mol/(cm^2 s)), indicating that the assumption of symmetrical flux decrease is valid in this case. When the S/P-6.4 layer is added to the BP-1, the i_{lim1} decreases further to 0.32 mA/cm^2. The measurement of the Cl^- for this laminate was not possible, because the values were below the detection limit of our method. However, using the i_{lim1} and the symmetrical flux decrease assumption like described above, we estimate that the Cl^- flux is 2.7×10^{-9} mol/(cm^2 s).

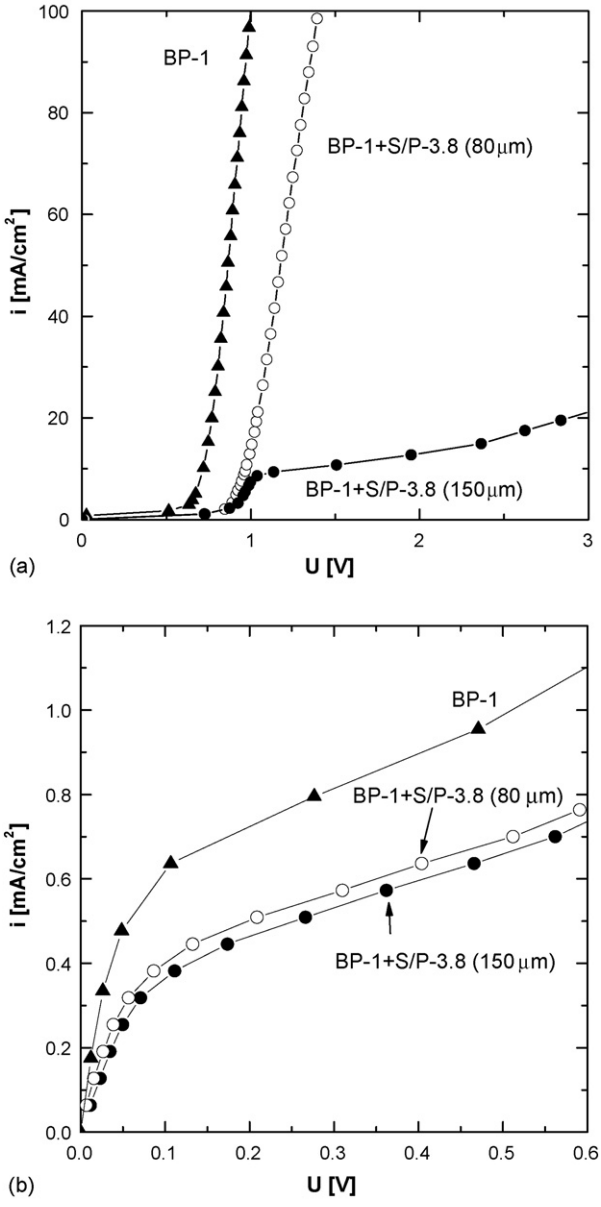

Fig. 7. i–v curves of BP-1 and BP-1 + S/P laminates, measured in 2 M NaCl. Influence of the layer thickness. (a) Full curves and (b) focusing at low current density.

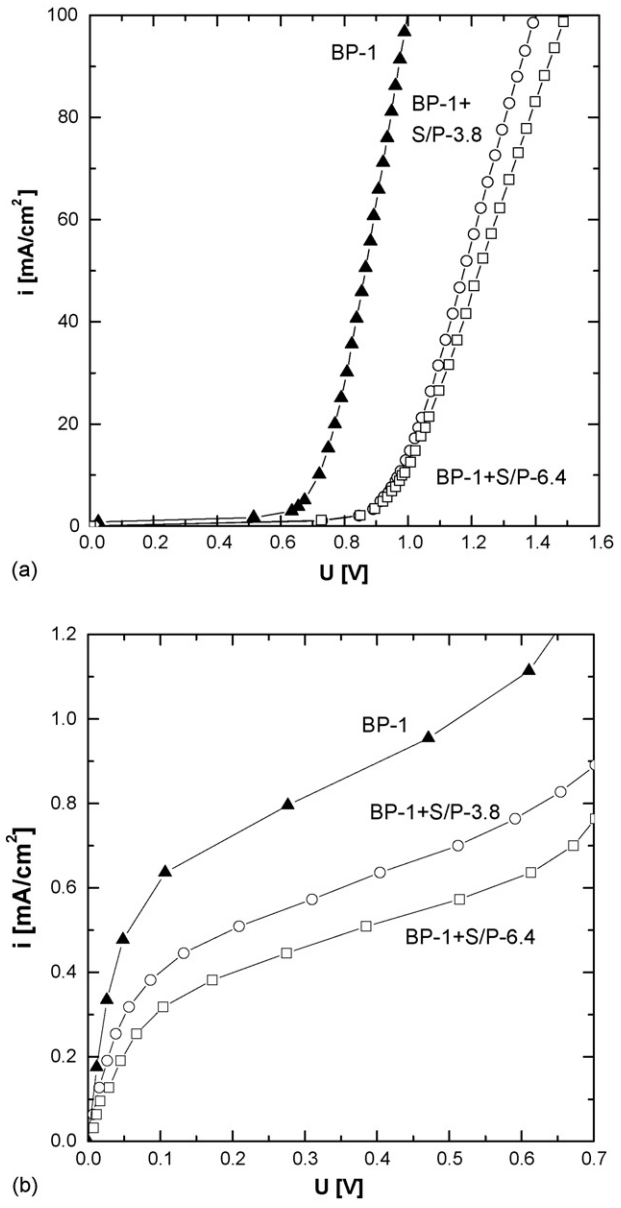

Fig. 8. *i–v* curves of BP-1 and BP-1 + S/P laminates, measured in 2 M NaCl. Influence of the layer composition. (a) Full curves and (b) focusing at low current density.

It seems that the charge density of the S/P blend has a significant impact on the BPM selectivity. The BP-1 + S/P-6.4 laminate has lower i_{lim1} and Cl^- leakage due to the Donnan exclusion mechanism.

It is important to note that the CMX and S/P-6.4 blend membrane have the same charge density (c_{char} = 6.4 mol/L, Tables 1–3) but the CMX membrane is thicker (163 μm in comparison to 65 μm of S/P-6.4). When laminated to the BP-1, they both cause nearly the same decrease of i_{lim1}. The thicker CMX membrane results in higher R_{op} and lower i_{lim2} in comparison to the S/P-6.4 (see Tables 2 and 4). This indicates that the achieved Cl^- leakage using the S/P-6.4 layer is probably close to the maximum achievable reduction through the cationic side of the BP-1. A further increase in the layer thickness of the cationic side of the BP-1 leads to water diffusion limitations.

In summary, the results of the modification of the BP-1 membrane show that the salt ion fluxes through the BP-1 can be reduced by the addition of extra layers. The reduction of the salt fluxes depends on the charge density and the thickness of the layers. The maximum reduction of Cl^- flux (47%) can be achieved with the BP-1 + S/P-6.4 laminate. Because the cationic layer of the BP-1 contains more water than the anionic side, the increase in CEL thickness leads to a strong reduction of the co-ion flux, but also to a reduction in water flux into the BP-1 and therefore to water diffusion limitations. In order to achieve lower co-ion leakages through the cationic side of a BPM, tailor made BPMs have to be prepared with thinner anion exchange layers to avoid water diffusion limitations.

4.2. Tailor made asymmetric BPMs

4.2.1. Effect of the AEL thickness

Tailor made BPMs were prepared as described in Section 3.2. The cation exchange layer was always the same (S/P-3.8, 80 μm) while the thickness of the anion exchange layer (aminated Psf) was varied. The interface layer was always a thin film of S-PEEK SD80 and P4VP. Fig. 9a shows the influence of the AEL thickness on the i_{lim1} and the shape of the plateau in the corresponding *i–v* curves. The i_{lim1} decreases with increasing AEL thickness, as expected. Additionally, the shape of the plateau is better defined (more horizontal) at high AEL thickness. The membrane with the very thin layer (0.4 μm) does not have a well-defined limiting current region. This is probably due to the high co-ion leakage through this layer [4]. With increasing the AEL thickness, the co-ion flux through the BPM and therefore the difference in co-ion depletion decreases, leading to a distinct plateau. Fig. 9b shows that both the i_{lim1} and the η_{NaOH} seem to reach a plateau for AEL thicker than 4–5 μm. In order to avoid high co-ion leakage and having better efficiency, AEL thickness higher than 5 μm should be used. To avoid water transport limitations, the AEL should not be too thick. Therefore a BPM having the 10 μm AEL is chosen for further investigations.

4.2.2. Effect of the CEL composition and thickness

In these experiments, the anion exchange layer was always the same (aminated Psf, 10 μm) while the composition and the thickness of the CEL was varied. Fig. 10a shows the *i–v* curves and Table 5 shows the i_{lim1} and Cl^- fluxes of asymmetric BPMs prepared using S/P-3.8 and S/P-6.4 blends as CEL (see Table 3). The BPM with the S/P-6.4 CEL has a lower i_{lim1} and a lower Cl^- flux compared to the BPM with the S/P-3.8 CEL. The Cl^- flux through the BPM with the S/P-6.4 CEL is 31% lower than the flux through the BPM with the S/P-3.8 CEL, while R_{op} increased about 23%.

Fig. 10b shows the *i–v* curves of BPMs containing S/P-3.8 CELs of different thickness. The membrane with 230 μm thickness has 62% lower i_{lim1} than the membrane with 80 μm thickness (5.6–14.6 mA/cm^2, respectively Table 5) and a 29% higher R_{op}. For the 230 μm S/P-3.8 membrane, the Cl^- flux was not detectable. However, if we use Eq. (3) (assuming symmetrical flux decrease), we estimate the Cl^- flux at 1.9 mol/(cm^2 s), Table 5).

Table 5
Influence of the cation exchange layer composition and thickness

CEL	d_{CEL} (μm)	i_{lim} (mA/cm^2)	R_{diss} (Ω cm^2)	R_{op} (Ω cm^2)	J_{Cl^-} ($\times 10^{-9}$ mol(cm^2 s))	
					Measured	Estimated
S/P-3.8	80	14.6	11.4	54.2	5.1	–
S/P-3.8	230	5.6	13.1	59.8	–	1.9
S/P-6.4	65	8.2	12.2	66.6	3.5	–

For the tailor made BPMs, it is interesting to check the applicability of Eq. (14), which relates the Cl^- flux to the layer thickness and c_{char}, and the comparison between estimated and measured Cl^- fluxes. Using the measured properties for the S/P-3.8 layer, (J_{Cl^-}, 5.1×10^{-9} mol/(cm^2 s); d_{wet}, 80 μm; c_{char}, 3.8 mol/L), Eq. (14) gives Cl^- diffusion coefficient ($D_{Cl^-,S/P}$) of 3.8×10^{-14} cm^2/s. Assuming that $D_{Cl^-,S/P}$ is the same for the S/P layers (all layers contain the same materials: 60% S-PEEK and 40% PES), one can get a master curve showing the dependence of J_{Cl^-} normalised for the c_{char} versus the membrane thickness (see Fig. 11). Our experimental (measured and estimated) J_{Cl^-} fluxes for the tailor made BPMs (see Table 5) follow nicely this master curve. This comparison shows that Eq.

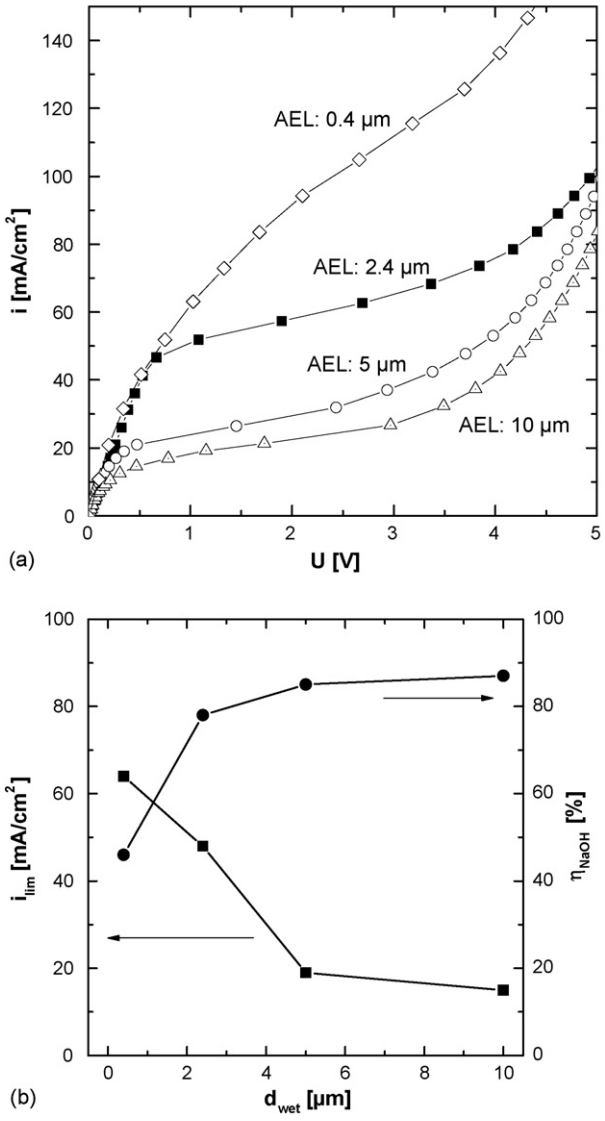

Fig. 9. Effect of the AEL layer thickness on the properties of tailor made BPMs with constant CEL, measured in 2 M NaCl. (a) *i–v* curves and (b) dependence of i_{lim1} and current efficiency on the AEL thickness.

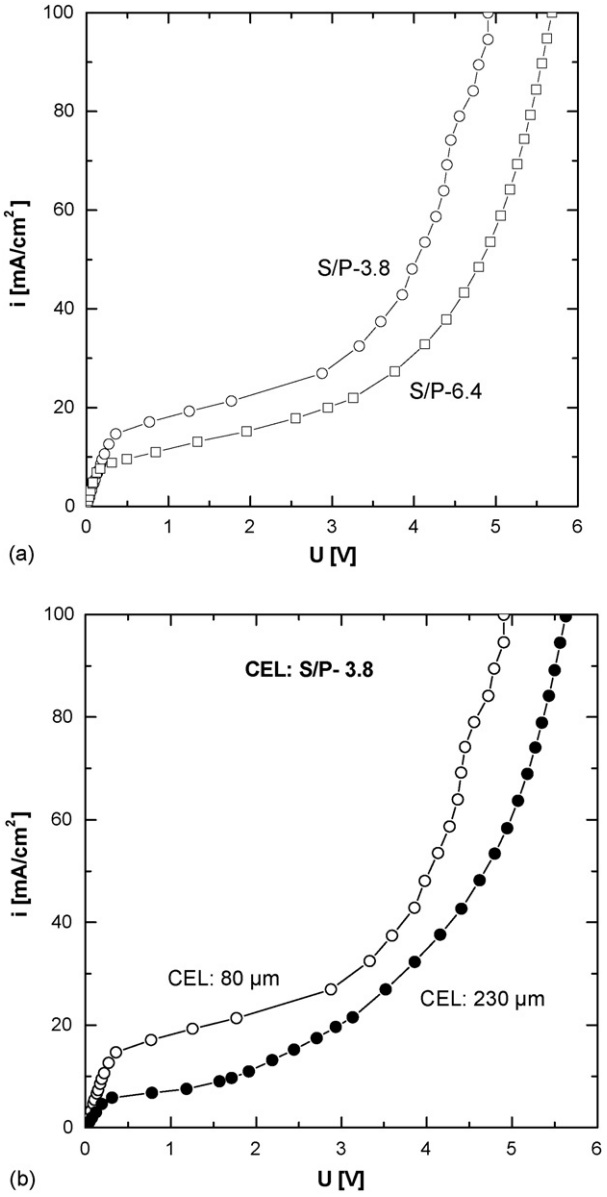

Fig. 10. Effect of the S/P blend properties of the *i–v* curve of tailor made BPMs with constant AEL, measured in 2 M NaCl. (a) Influence of charge density and (b) influence of layer thickness.

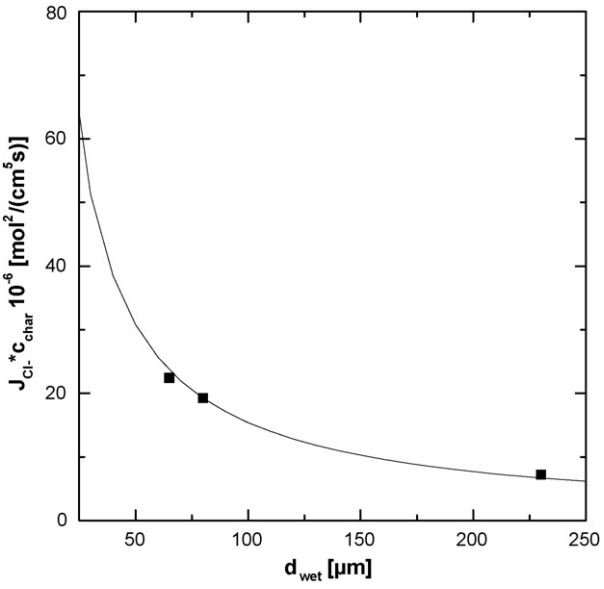

Fig. 11. Dependence of J_{Cl^-} normalised for c_{char} on d_{wet} of the S/P CEL. Comparison of the calculated (line based on Eq. (14)) and experimental fluxes (symbols).

(14) is suitable to predict well the properties of the tailor made BPM and can be used as a tool to design a BPM with tailor made properties and selectivity.

In summary, the tailor made BPMs show a reduced Cl^- leakage compared to the commercial BP-1 membrane. The Cl^- leakage depends on the charge density and the thickness of the CEL and can be predicted by the master curve based on Eq. (14). Because of the thin AEL (10 μm) and therefore the high water flux through the anionic side of the BPM, the thickness of the CEL could be increased to 230 μm without having water diffusion limitations. The principle of asymmetry can therefore be used to tailor BPMs to achieve high purity products at one side of the BPM process, while reducing the purity of the product at the other side.

5. Conclusions

In this work, we have shown that BPM asymmetry can be used to decrease the co-ion fluxes through the BPM. The thickness and charge density determine the co-ion leakage through the corresponding ion exchange layer.

Experiments with the commercial BP-1 membrane have shown that the cationic side of the membrane contains much more water and more co-ions than the anionic side. Therefore the limiting current density is more affected by the lamination of CELs. The addition of a thin S/P-6.4 CEL (65 μm) onto the cationic side of the BP-1 membrane (BP-1 + S/P-6.4) produced the best BPM with a decrease in co-ion leakage of 47%.

Tailor made BPMs have also been prepared showing a reduced Cl^- leakage compared to the commercial BP-1 membrane. The Cl^- leakage depends on the charge density and the thickness of the CEL. Because of the thin AEL (10 μm) and therefore the high water flux through the anionic side of the BPM, the thickness of the CEL (S/P-3.8) could be increased to 230 μm leading to low Cl^- flux without water diffusion limitations.

The increase in bipolar membrane asymmetry decreases the co-ion leakage, but also causes an increase in membrane resistance leading to higher energy consumption for the production of acids and bases. However, the decrease in co-ion leakage and therefore the increase in product purity are higher than the corresponding increase in membrane resistance.

Acknowledgement

This project is financially supported by the Netherlands organisation for scientific research (NWO-CW/STW, Project no: 5739).

List of symbols

A	membrane area (m^2)
AEL	anion exchange layer (also as subscript)
BPM	bipolar membrane
c	concentration (mol/L)
c_{char}	charge density (mol/L)
CEL	cation exchange layer (also as subscript)
Cond	conductivity (mS/cm)
d_{wet}	thickness of the wet membrane layer (μm)
D	diffusion coefficient (m^2/s)
ED-BPM	bipolar membrane electrodialysis
F	Faraday constant (96,485 A s/mol)
i	applied current density (A/m^2)
I	applied current (A)
IEC	ion exchange capacity (mol/kg_{dry})
IEL	ion exchange layer
J	flux (mol/(m^2 s))
M^+	salt or base cation (also as subscript)
N	number of repeat units
NMP	*N*-methyl-2-pyrrolidinone
P	permselectivity (%)
PEEK	poly(ether ether ketone)
PES	poly(ether sulfone)
Psf	polysulfone
P4VP	poly-(4-vinyl pyridine)
R	area resistance (Ω cm^2)
S-PEEK	sulphonated poly(ether ether ketone)
S/P	S-PEEK/PES blend, 60/40 (also as subscript)
SD	sulphonation degree (%)
t	time (s)
t_{Cl^-}	transport number of chloride (%)
T	temperature (K)
U	potential difference (V)
V	Circulated volume (L)
w	water uptake (kg_{water}/kg_{dry})
x	location normal to the membrane (m)
X^-	salt or acid anion (also as subscript)
z	valence

Greek symbol

η	current efficiency (%)

Superscripts/subscripts

0	at time zero
av	arithmetic average
diss	dissociation
i	species i
lim	limiting
m	membrane phase
op	operational
s	at the solution side
t	at given production time

References

[1] J. Balster, D.F. Stamatialis, M. Wessling, Electro-catalytic membrane reactors and the development of bipolar membrane technology, Chem. Eng. Proc. 43 (2004) 1115–1127.

[2] F.G. Wilhelm, N.F.A. van der Vegt, M. Wessling, H. Strathmann, Bipolar membrane preparation, in: A.J.B. Kemperman (Ed.), Bipolar Membrane Handbook, Twente University Press, Enschede, The Netherlands, 2000.

[3] R. El Moussaoui, G. Pourcelly, M. Maeck, H.D. Hurwitz, C. Gavach, Co-ion leakage through bipolar membranes, influence ion *I–V* responses and water-splitting efficiency, J. Membr. Sci. 90 (1994) 283–292.

[4] F.G. Wilhelm, I. Punt, N.F.A. van der Vegt, M. Wessling, H. Strathmann, Optimisation strategies for the preparation of bipolar membranes with reduced salt ion leakage in acid–base electrodialysis, J. Membr. Sci. 182 (2001) 13–28.

[5] F.G. Wilhelm, I. Punt, N.F.A. van der Vegt, M. Wessling, H. Strathmann, Asymmetric bipolar membranes in acid–base electrodialysis, Ind. Eng. Chem. Res. 41 (2002) 579–586.

[6] T. Aritomi, T. van der Boomgaard, H. Strathmann, Current voltage curve of a bipolar membrane at high current density, Desalination 104 (1996) 13–18.

[7] J.J. Krol, M. Jansink, M. Wessling, H. Strathmann, Behaviour of bipolar membranes at high current density: water diffusion limitation, Sep. Purif. Technol. 14 (1998) 41–52.

[8] J.L. Gineste, G. Pourcelly, Y. Lorrain, F. Persin, C. Gavach, Analysis of factors limiting the use of bipolar membranes: a simplified model to determine trends, J. Membr. Sci. 112 (1996) 199–208.

[9] D. Raucq, G. Pourcelly, C. Gavach, Production of sulphuric acid and caustic soda from sodium sulphate by electromembrane processes. Comparison between electro-electrodialysis and electrodialysis on bipolar membrane, Desalination 91 (1993) 163–175.

[10] T.A. Davis, T. LaTerra, On-site generation of acid and base with bipolar membranes: a new alternative to purchasing and storing regenerants, in: Proceedings of the 48th Annual Meeting of the International Water Conference, 1987.

[11] R. Simons, Preparation of a high performance bipolar membrane, J. Membr. Sci. 78 (1993) 13–23.

[12] J. Balster, O. Krupenko, I. Pünt, D.F. Stamatialis, M. Wessling, Preparation and characterisation of monovalent ion selective cation exchange membranes based on sulphonated poly(ether ether ketone), J. Membr. Sci. 263 (2005) 137–145.

[13] F.G. Wilhelm, I.G.M. Punt, N.F.A. van der Vegt, H. Strathmann, M. Wessling, Cation permeable membranes from blends of sulfonated poly(ether ether ketone) and poly(ether sulfone), J. Membr. Sci. 199 (2002) 167–176.

[14] B. Bauer, Bipolare Mehrschichtmembranen (bipolar multilayer membranes), Fraunhofer-Gesellschaft zur Förderung der Angewandten Forschung e.V (FhG) (Germany), DE Patent 4026154 (1992).

[15] J.J. Krol, M. Wessling, H. Strathmann, Concentration polarization with monopolar ion exchange membranes: current–voltage curves and water dissociation, J. Membr. Sci. 162 (1999) 145–154.

[16] X. Tongwen, Y. Weihua, Effect of cell configurations on the performance of citric acid production by a bipolar membrane electrodialysis, J. Membr. Sci. 203 (2002) 145–153.